

# Spin Reversal of a Rattleback with Viscous Friction

Hiroshi Takano\*

*Joetsu university of education,  
Joetsu, Niigata, 943 Japan*

Received August 29, 2013; accepted November 12, 2013

**Abstract**—An effective equation of motion of a rattleback is obtained from the basic equation of motion with viscous friction depending on slip velocity. This effective equation of motion is used to estimate the number of spin reversals and the rattleback's shape that causes the maximum number of spin reversals. These estimates are compared with numerical simulations based on the basic equation of motion.

MSC2010 numbers: 70E18, 70F40

DOI: 10.1134/S1560354714010067

Keywords: rattleback, viscous friction

## 1. INTRODUCTION

A rattleback, also known as a celt or wobblestone, is a type of mechanical top with the curious property of spin asymmetry. Nowadays, there are different varieties of rattlebacks. Figure 1 shows a Russian rattleback toy called stubborn tortoise. When the rattleback is spun in the clockwise direction which the tortoise has been turned to, it continues to spin clockwise until it slows to a stop. However, when the rattleback is spun in the anticlockwise direction, a self-induced oscillation occurs, and the spin slows down and eventually its direction is reversed. There is an inertial asymmetry, because the tortoise's center of mass is shifted from the principal axes of the body surface ellipsoid. This inertial asymmetry is responsible for spin reversal.



**Fig. 1.** A Russian rattleback toy called stubborn tortoise.

Many analyses and simulations have attempted to explain the dynamics of rattlebacks during the last century.

The first scientific paper on rattlebacks appeared in 1898 (Walker [1]). Assuming dissipation-free rolling without slipping, he obtained linearized equations of motion for contact point coordinate variables and spin variables. He analyzed the instability of the spin magnitude and direction by studying a characteristic equation and showed the relationship between the direction of spin and the oscillation.

\*E-mail: takano@juen.ac.jp

In 1983, Pascal [2], using the same assumptions as Walker [1], derived effective equations of motion for the slowly varying mode by using the method of averaging and clarified a rattleback's reversal mechanism.

During the same period, Markeev [3] obtained results similar to that of Pascal [2]. He derived two conservation laws and provided a comprehensible explanation of a rattleback's reversal. Their results were extended to second-order averaging by Blackowiak, Rand and Kaplan [4].

Moffatt and Tokieda [5] presented a physically transparent derivation of the effective equations of motion similar to Markeev's derivation.

In 1986, Bondi [6] extended Walker's [1] results to understand how spin evolves for a wide range of geometric and inertial parameters of the body.

Recently, strange attractors and new effects in rattleback dynamics are studied by Borisov et.al. [7–9].

For a no-slip dissipation-free case, numerical simulations [10–12] showed that infinite spin reversals occur. On the other hand, real rattleback has finite spin reversals because of energy loss by slip friction. Thus, it is important to analyze the dynamics of rattlebacks with slip friction.

Karapetian [13] discussed the stability of rotation of a heavy asymmetric rigid body (rattleback) on a horizontal plane with viscous friction, but did not mention the number of spin reversals discussed in this paper.

Garcia and Hubbard [12] discussed the limitations of a no-slip case and analyzed the effects of dissipation. They derived augmented equations of motion incorporating lumped models for aerodynamic effects, spinning torque and slipping torque due to Coulomb friction force of slip velocity. In reality, the contact with the horizontal plane is not a point but an area, and relative angular motion between the surfaces causes spinning torque and slipping torque. These equations were solved numerically. Because these equations were too complicated, they presented a simplified model of spin.

The spin model derived by considering energy in the spin, oscillation, and dissipation was successful in explaining spin dynamics, this model was not derived from equations of motion. Thus, the effect of the slip velocity is not clear. Furthermore, they did not discuss the number of spin reversals and its relationship to the rattleback's shape.

The observation of the actual behavior of rattlebacks leads to three questions.

First, for the no-slip case, if the initial spin value  $n_0$  is small, the rattle oscillation becomes large and spin reversal occurs in theory. In contrast, for the slip case, if  $n_0$  is small, the rattle oscillation does not increase, and spin reversal does not occur. In this case, a critical value of the initial spin  $n_c$  seems to exist, above which the spin reversal occurs. What is the value of  $n_c$ ?

Second, a real rattleback has a finite number of spin reversals because of energy loss due to slip friction. When the value of the coefficient of friction is known, how many times does the rattleback reverse and how does the number of spin reversals depend on the coefficient of friction?

Third, it seems that the number of spin reversals depends on the rattleback's shape. One rattleback may reverse only once, whereas another may reverse as many as three times. Given that the lower surface of the rattleback is defined by an ellipsoid  $\frac{x^2}{a^2} + \frac{y^2}{b^2} + \frac{z^2}{c^2} = 1$ , where  $a > b > c = 1$ , if  $a \gg b$ , the oscillations in the  $x$  direction become large and spin reversal occurs rapidly. After one reversal, the oscillations start in the  $y$  direction but do not become as large, and spin reversal occurs slowly. In this situation, the number of spin reversals is small. In contrast, if  $a = b$ , the rattleback is a disk, and spin reversals do not occur. Thus, it seems that a critical ratio of  $a$  and  $b$  gives the maximum number of spin reversals. What is this value?

In this paper, to answer the above questions, I consider the basic equations of motion containing sliding friction and obtain linearized equations of motion containing slip velocity. I derive the effective equations of motion by approximating this velocity. By applying the same averaging method as that used by Pascal [2], differential equations of slowly changing variables are obtained. These differential equations are used to analyze the relationship among the number of spin reversals, the coefficient of friction, and the rattleback's shape. The spin behavior obtained from the simulation of the effective equations of motion is compared with that obtained from the simulation of basic equations of motion.

2. BASIC EQUATIONS OF MOTION FOR A RATTLEBACK WITH VISCOUS FRICTION

In this paper, a rattleback is considered to be a uniform ellipsoid of mass  $m$  with a smooth lower surface such that  $a > b > c$  as follows:

$$\frac{\tilde{x}^2}{a^2} + \frac{\tilde{y}^2}{b^2} + \frac{\tilde{z}^2}{c^2} = 1,$$

where  $\tilde{x}$ ,  $\tilde{y}$ , and  $\tilde{z}$  are the body axes of the rattleback as shown in Fig. 2. The distances of the three axes from the center of mass are  $a$ ,  $b$ , and  $c$ , respectively. The principal inertia axes are  $x$ ,  $y$ , and  $z$ . The  $z$ -axis is directed downward and coincides with the  $\tilde{z}$ -axis. The  $x$ - and  $y$ -axes are rotated by angle  $\delta$  such that

$$\begin{pmatrix} \tilde{x} \\ \tilde{y} \end{pmatrix} = \begin{pmatrix} \cos \delta & -\sin \delta \\ \sin \delta & \cos \delta \end{pmatrix} \begin{pmatrix} x \\ y \end{pmatrix},$$

$$\tilde{z} = z.$$

In this paper, it is assumed that  $\delta$  is small, such as  $O(10^{-2})$ . The vector at the contact point  $P$ ,  $\mathbf{x}_p$ , has components  $x$ ,  $y$ , and  $z$ .  $\mathbf{u}$  is the upward unit vector at point  $P$ .

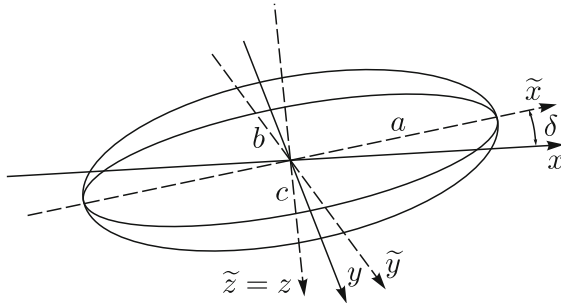


Fig. 2. Body axes  $\tilde{x}$ ,  $\tilde{y}$ , and  $\tilde{z}$  with lengths  $a$ ,  $b$ , and  $c$ , respectively, principal inertia axes  $x$ ,  $y$ ,  $z$  and angle  $\delta$ .

When the rattleback rotates, point  $P$  is near the point  $(0, 0, c)$ . When the rattleback oscillates, the values of  $x$ ,  $y$  are  $|x| < a$  and  $|y| < b$ , respectively, and  $z$  can be expanded by a second-order approximation of  $\frac{x}{a} < 1$  and  $\frac{y}{b} < 1$  as follows:

$$z \simeq c \left( 1 - \left\{ \frac{p}{2} \left( \frac{x}{c} \right)^2 + q \frac{xy}{c^2} + \frac{s}{2} \left( \frac{y}{c} \right)^2 \right\} \right),$$

where the parameters  $p$ ,  $q$ , and  $s$  are given by

$$p \equiv c^2 \left( \frac{\cos^2 \delta}{a^2} + \frac{\sin^2 \delta}{b^2} \right), \tag{2.1}$$

$$q \equiv c^2 \cos \delta \sin \delta \left( \frac{1}{b^2} - \frac{1}{a^2} \right), \tag{2.2}$$

$$s \equiv c^2 \left( \frac{\sin^2 \delta}{a^2} + \frac{\cos^2 \delta}{b^2} \right). \tag{2.3}$$

At the leading order, the following equations are obtained:

$$\mathbf{x}_p \simeq (x, y, c), \tag{2.4}$$

$$\mathbf{u} \simeq \left( -\frac{px + qy}{c}, -\frac{qx + sy}{c}, -1 \right). \tag{2.5}$$

Assuming that  $\delta$  is small, the principal moments of inertia  $I_{10}$ ,  $I_{20}$ , and  $I_{30}$  are approximated as follows:

$$I_{10} \simeq mI_1, \quad I_{20} \simeq mI_2, \quad I_{30} \simeq mI_3,$$

where

$$I_1 \equiv \frac{b^2 + c^2}{5c^2}, \quad I_2 \equiv \frac{a^2 + c^2}{5c^2}, \quad I_3 \equiv \frac{a^2 + b^2}{5c^2}.$$

In the following equations, the basic equations of motion for the angular momentum  $\mathbf{L}$  and the velocity of the center of mass  $\mathbf{v}_g$  are shown. In Section 6, numerical simulations of these basic equations of motion are performed. The evolution of angular momentum is governed by Euler's equation:

$$\frac{d}{dt}\mathbf{L} = \mathbf{x}_p \times (R\mathbf{f} + R\mathbf{u}), \quad (2.6)$$

where  $R\mathbf{u}$  is the normal reaction at  $P$ , and  $R\mathbf{f}$  is the slip friction force at  $P$ . The dynamics of the center of mass is governed by Newton's equation for the center of mass velocity  $\mathbf{v}_g$ :

$$m\frac{d}{dt}\mathbf{v}_g = (R - mg)\mathbf{u} + R\mathbf{f}. \quad (2.7)$$

The slip velocity,  $\mathbf{v}_p$ , is related to velocities  $\mathbf{v}_0 \equiv \mathbf{x}_p \times \boldsymbol{\omega}$  and  $\mathbf{v}_g$  as follows:

$$\mathbf{v}_p = \mathbf{v}_g - \mathbf{v}_0. \quad (2.8)$$

Because  $\mathbf{f}$ ,  $\mathbf{v}_p$ , and  $\frac{d}{dt}\mathbf{v}_p$  only have components in the horizontal direction, using Eqs. (2.7) and (2.8), the normal reaction  $R$  is given by

$$R = mg + m \left( \frac{d}{dt}\mathbf{v}_0 \right) \cdot \mathbf{u}. \quad (2.9)$$

The Coulomb law is often used to define sliding friction as follows:

$$\mathbf{f} = -\mu_c \frac{\mathbf{v}_p}{|\mathbf{v}_p|},$$

where  $\mathbf{v}_p$  is the slip velocity and  $\mu_c$  is the coefficient of Coulomb friction. It is difficult to analyze the equations of motion because this definition of the Coulomb friction is undefined at  $\mathbf{v}_p = 0$ . Thus, in this paper, viscous friction is adopted to perform a first examination of spin reversal. Viscous friction is linearly related to  $\mathbf{v}_p$  as follows:

$$\mathbf{f} = -\mu\mathbf{v}_p \quad (2.10)$$

where  $\mu$  is the coefficient of viscous friction with unit  $s/cm$ . It is found that viscous friction is well defined at  $\mathbf{v}_p = 0$ . The angular momentum  $\mathbf{L}$  has components in the principal inertia axes as follows

$$\mathbf{L} = (I_{10}\omega_1, I_{20}\omega_2, I_{30}\omega_3),$$

where  $\omega_i$  are the components of the angular velocity  $\boldsymbol{\omega}$  of the rattleback.  $\boldsymbol{\omega}$  is given by the equation  $\frac{d}{dt}\mathbf{u} = 0$ . In general, because the unit vectors of the principal inertia axes  $\mathbf{e}_i$  have time dependence, the time derivative of the vector  $\mathbf{A}$  is given by

$$\frac{d}{dt}\mathbf{A} = \frac{\partial}{\partial t}\mathbf{A} + (\boldsymbol{\omega} \times \mathbf{A}),$$

where  $\frac{\partial}{\partial t}\mathbf{A} \equiv (\frac{d}{dt}A_i)\mathbf{e}_i$ . Then

$$\boldsymbol{\omega} = \frac{\partial}{\partial t}\mathbf{u} \times \mathbf{u} + n\mathbf{u}, \quad (2.11)$$

where  $n \equiv \boldsymbol{\omega} \cdot \mathbf{u}$ . The dynamical variables of these basic equations of motion are the components of the angular velocity  $\omega_i$  and the slip velocity  $v_{pi}$ .

The equations of motion are obtained by dividing both sides of Eqs. (2.6) and (2.7) by  $g$  and rescaling of the variables as follows:

$$\begin{aligned}\tilde{t} &= \sqrt{g}t, & \tilde{\mathbf{L}} &= \frac{\mathbf{L}}{\sqrt{g}}, & \tilde{\boldsymbol{\omega}} &= \frac{\boldsymbol{\omega}}{\sqrt{g}}, \\ \tilde{R} &= \frac{R}{g}, & \tilde{\mathbf{v}}_p &= \frac{\mathbf{v}_p}{\sqrt{g}}, & \tilde{\mu} &= \sqrt{g}\mu.\end{aligned}$$

In addition, the length of  $c$  is assumed to be unit length, i.e.,  $c = 1\text{cm}$  thus  $c$  does not appear in equations in the remaining sections.

When a rattleback is turned slightly by hand such that the initial value of rotation is  $\simeq 2\pi$  rad/s, spin reversal occurs. Because gravitational constant takes the value  $g \simeq 980$  cm/s<sup>2</sup>, the spin value is  $\tilde{n} \simeq 0.201$ . As spin reversal occurs at this spin value or lower spin values, the order of  $\tilde{n}$  such as  $\tilde{n} = \frac{n}{\sqrt{g}} \simeq O(10^{-2})$  may be assumed. This assumption is the same as that for the neighborhood of the position of stable equilibrium discussed by Pascal[2]. The value of the order of  $\tilde{n} \simeq O(10^{-2})$  is used in the next section to approximate the equations of motion.

In the case of limiting  $\mu$  to infinity, these equations of motion lead to the no-slip case, as shown by the numerical simulation performed in Section 6. Therefore, to consider a case in which spin reversal occurs several times,  $\mu$  is assumed to be not as small as  $\tilde{\mu} \simeq O(10^2) \simeq \frac{1}{\tilde{n}}$ .

In the remaining sections, the tilde symbol above the variables is omitted.

### 3. EFFECTIVE EQUATIONS OF MOTION

This section shows that the effective equations of motion for a rattleback are obtained by applying the same linearization method as that of Walker [1] and Pascal [2],

The parameters  $c$  and  $n$  are set 1 and  $\simeq \frac{1}{\mu} \simeq O(10^{-2})$ , respectively, as discussed in the previous section.

The contact point  $\mathbf{x}_p$  has components  $(x, y, z)$ , which satisfy  $\frac{|x|}{a} < 1$ ,  $\frac{|y|}{b} < 1$ . The second-order terms can be neglected. Assuming that  $\delta \simeq O(10^{-2})$ ,  $a \simeq O(10)$ , and  $b \simeq O(1)$ , Eqs. (2.1), (2.2), and (2.3) for the parameters  $p$ ,  $q$ , and  $s$  are, respectively, approximated as

$$p \simeq \frac{1}{a^2}, \quad q \simeq \frac{\delta}{b^2}, \quad s \simeq \frac{1}{b^2}.$$

These equations imply that the second-order terms of  $\sqrt{p}x$ ,  $\sqrt{s}y$ ,  $\sqrt{q}x$ , and  $\sqrt{q}y$  can be neglected. In addition, the order of the spin value  $n \simeq O(10^{-2})$  is used, as discussed in the previous section. The second-order terms of  $n$ ,  $p$ ,  $s$ , and  $q$  are also neglected.

For the orders of  $\dot{x}$  and  $\dot{y}$ , when the time derivative of  $x$  is considered,  $x$  is multiplied by the oscillation factor. Because a rattleback, unlike a usual top, does not oscillate rapidly,  $x$  and  $\dot{x}$  are assumed to have the same order. In fact, as Eqs. (3.37) and (3.38) will show, the oscillations are almost  $\cos(\nu_{1,2}t)$ , and according to Eqs. (3.23) and (3.24),  $\nu_1^2 \simeq \frac{5a^2}{a^2+6}$  and  $\nu_2^2 \simeq \frac{5b^2}{b^2+6}$ , respectively. When  $a = 10$  and  $b = 3$ , as assumed in the simulation in Section 6,  $\nu_{1,2}$  are  $\nu_1^2 \simeq 5$  and  $\nu_2^2 \simeq 3$ ; thus, it is assumed that  $\nu_{1,2} \simeq O(1)$ . Therefore, the second-order terms of  $O(\dot{x}) \simeq O(x)$ , and  $O(\dot{y}) \simeq O(y)$ , such as  $psx\dot{y}$  are neglected.

In this approximation, by using Eqs. (2.4), (2.5), and (2.11),  $\boldsymbol{\omega} = (\omega_1, \omega_2, \omega_3)$  has the following components,

$$\boldsymbol{\omega} \simeq (q\dot{x} + s\dot{y}, -p\dot{x} - q\dot{y}, -n), \quad (3.1)$$

and  $\mathbf{v}_0 = \mathbf{x}_p \times \boldsymbol{\omega}$  has components

$$\mathbf{v}_0 \simeq (p\dot{x} + q\dot{y} - ny, q\dot{x} + s\dot{y} + nx, 0). \quad (3.2)$$

Because the second term of the time derivative of  $\mathbf{v}_0$ ,  $\boldsymbol{\omega} \times \mathbf{v}_0$ , is second order of  $n$ ,  $p$ ,  $q$  and  $s$ ,  $\frac{d}{dt}\mathbf{v}_0$  are as follows:

$$\begin{aligned} \frac{d}{dt}\mathbf{v}_0 &\simeq \frac{\partial}{\partial t}\mathbf{v}_0 \\ &\simeq (p\ddot{x} + q\ddot{y} - n\dot{y}, q\ddot{x} + s\ddot{y} + n\dot{x}, 0), \end{aligned} \quad (3.3)$$

where terms such as  $\dot{n}y$  are neglected because  $\dot{n}$  is a second-order term, as will be shown in Eq. (3.15).

In Eq. (2.9) for  $R$ , it is seen from Eqs. (2.5) and (3.3) that  $(\frac{d}{dt}\mathbf{v}_0) \cdot \mathbf{u}$  is a second-order term; thus,  $R \simeq m$ . Therefore, setting  $R = m$  in Eqs. (2.6) and (2.7), the following equations are obtained

$$\frac{d}{dt}\mathbf{L} = m(\mathbf{N}_0 + \mathbf{N}_g + \mathbf{N}_p), \quad (3.4)$$

$$\frac{d}{dt}\mathbf{v}_g = \mathbf{f}, \quad (3.5)$$

where

$$\mathbf{N}_0 \equiv \mathbf{x}_p \times \frac{d}{dt}\mathbf{v}_0, \quad \mathbf{N}_g \equiv \mathbf{x}_p \times \mathbf{u}, \quad \mathbf{N}_p \equiv \mathbf{x}_p \times \frac{d}{dt}\mathbf{v}_p.$$

These equations contain six dynamical variables:  $x$ ,  $y$ ,  $n$ , and the components of  $\mathbf{v}_p$ . Therefore, it is difficult to analyze the dynamics of these variables.

Using the approximation in Eq. (3.1) for  $\boldsymbol{\omega}$ , and neglecting the second-order terms of  $n$ ,  $p$ ,  $q$  and  $s$ , the approximation of  $\frac{d}{dt}\mathbf{L}$  has components

$$\frac{d}{dt}\mathbf{L} \simeq (I_1(q\ddot{x} + s\ddot{y}), -I_2(p\ddot{x} + q\ddot{y}), -I_3\dot{n}). \quad (3.6)$$

At the leading order,  $\mathbf{N}_0$  has components

$$\begin{aligned} N_{01} &\simeq -(q\ddot{x} + s\ddot{y}) - n\dot{x}, \\ N_{02} &\simeq p\ddot{x} + q\ddot{y} - n\dot{y}, \\ N_{03} &\simeq q(x\ddot{x} - y\ddot{y}) + sx\ddot{y} - p\ddot{x}y + n(x\dot{x} + y\dot{y}), \end{aligned} \quad (3.7)$$

where the approximation  $n(1-p)x\dot{x} \simeq nx\dot{x}$  is adopted. At the leading order,  $\mathbf{N}_g$  has components

$$\mathbf{N}_g \simeq (-y, x, q(y^2 - x^2) + xy(p - s)), \quad (3.8)$$

where the approximation  $qx - (1-s)y \simeq -y$  is adopted.

The next thing to be discussed is an approximation in which  $\mathbf{v}_p$  is expressed by  $x$ ,  $y$ , and  $n$ . This approximation is crucial for simplifying these complicated equations of motion. Equations (2.8), (2.10), and (3.5) give  $\mu\mathbf{v}_p = -\frac{d}{dt}\mathbf{v}_0 - \frac{d}{dt}\mathbf{v}_p$ . In addition, the numerical simulation in Section 6 shows that  $\frac{d}{dt}\mathbf{v}_0 \gg \frac{d}{dt}\mathbf{v}_p$ . Thus, the following approximation is obtained:

$$\mathbf{v}_p \simeq -\frac{1}{\mu} \frac{d}{dt}\mathbf{v}_0. \quad (3.9)$$

Because the components of  $\mathbf{v}_0$  are given by  $x$ ,  $y$ , and  $n$  from Eq. (3.2), the dynamical variables reduce to  $x$ ,  $y$ , and  $n$  as will be shown in Eqs. (3.18)–(3.20). It is easily seen from Eqs. (3.3) and (3.9) that  $v_{p3}$  is a second-order term. In addition, the term  $\boldsymbol{\omega} \times \mathbf{v}_p$  is neglected in the time derivative of  $\mathbf{v}_p$ . Thus,  $\frac{d}{dt}\mathbf{v}_p$  has components,

$$\frac{d}{dt}\mathbf{v}_p \simeq \frac{\partial}{\partial t}\mathbf{v}_p \simeq (\dot{v}_{p1}, \dot{v}_{p2}, 0). \quad (3.10)$$

Using Eq. (3.10),  $\mathbf{N}_p$  has components

$$\mathbf{N}_p \simeq (-\dot{v}_{p2}, \dot{v}_{p1}, x\dot{v}_{p2} - y\dot{v}_{p1}). \quad (3.11)$$

Substituting Eqs. (3.6)–(3.11) into Eq. (3.4) gives

$$J_1(q\ddot{x} + s\ddot{y}) + n\dot{x} + y + \dot{v}_{p2} = 0, \quad (3.12)$$

$$J_2(p\ddot{x} + q\ddot{y}) - n\dot{y} + x + \dot{v}_{p1} = 0, \quad (3.13)$$

where

$$J_1 \equiv I_1 + 1 = \frac{b^2 + 6}{5}, \quad J_2 \equiv I_2 + 1 = \frac{a^2 + 6}{5}. \quad (3.14)$$

For  $\dot{n}$ , the following equation is obtained

$$I_3\dot{n} + q(x\ddot{x} - y\ddot{y}) + sx\ddot{y} - p\ddot{x}y + n(x\dot{x} + y\dot{y}) + (q(y^2 - x^2) + (p - s)xy) + x\dot{v}_{p2} - y\dot{v}_{p1} = 0. \quad (3.15)$$

Let  $v_{p1}, v_{p2}$  be expressed with respect to  $x, y$  and  $n$  from Eq. (3.9). Using Eqs. (3.3) and (3.13) and adopting approximations  $(1 - \frac{1}{J_2}) \simeq 1$  and  $\frac{\dot{v}_{p1}}{\mu} \simeq O(\frac{1}{\mu^2}) \simeq 0$  from Eq. (3.9),  $v_{p1}$  is given by

$$\begin{aligned} v_{p1} &\simeq -\frac{1}{\mu}(p\ddot{x} + q\ddot{y} - n\dot{y}), \\ &= -\frac{1}{\mu} \left( \frac{1}{J_2}(n\dot{y} - x - v_{p1}) - n\dot{y} \right), \\ &\simeq \frac{1}{\mu} \left( n\dot{y} + \frac{x}{J_2} \right). \end{aligned} \quad (3.16)$$

Similarly,  $v_{p2}$  is given by

$$v_{p2} \simeq -\frac{1}{\mu} \left( n\dot{x} - \frac{y}{J_1} \right). \quad (3.17)$$

By substituting Eqs. (3.16) and (3.17) into Eqs. (3.12)–(3.15), and neglecting  $O(\frac{n}{\mu}) (< O(q))$  terms, such as

$$\left( J_1q - \frac{n}{\mu} \right) \ddot{x} \simeq J_1q\ddot{x},$$

at the leading order, the following equations are obtained

$$J_1(q\ddot{x} + s\ddot{y}) + n\dot{x} + y + \frac{\dot{y}}{J_1\mu} = 0, \quad (3.18)$$

$$J_2(p\ddot{x} + q\ddot{y}) - n\dot{y} + x + \frac{\dot{x}}{J_2\mu} = 0, \quad (3.19)$$

$$I_3\dot{n} + q(x\ddot{x} - y\ddot{y}) + sx\ddot{y} - p\ddot{x}y + n(x\dot{x} + y\dot{y}) + (q(y^2 - x^2) + (p - s)xy) + \frac{x\dot{y}}{\mu J_1} - \frac{y\dot{x}}{\mu J_2} = 0. \quad (3.20)$$

From the above expressions, it is observed that the main parts are oscillations of  $x$  and  $y$ , such as  $\ddot{y} + \frac{1}{J_1s}y = 0$  and  $\ddot{x} + \frac{1}{J_2p}x = 0$ . Moffatt and Tokieda [5] suggested that the terms  $J_1q\ddot{x}$ ,  $n\dot{x}$ ,  $J_2q\ddot{y}$  and  $n\dot{y}$  are crucial in creating reverse oscillations. The effect of friction is included in the terms  $\frac{\dot{y}}{J_1\mu}$  and  $\frac{\dot{x}}{J_2\mu}$ .

Furthermore, to eliminate terms depending on  $q\ddot{x}$  and  $q\ddot{y}$ , the new variables  $X$  and  $Y$  are defined as follows:

$$\begin{pmatrix} X \\ Y \end{pmatrix} \equiv TJP \begin{pmatrix} x \\ y \end{pmatrix}, \quad (3.21)$$

where

$$J \equiv \begin{pmatrix} \sqrt{J_2} & 0 \\ 0 & \sqrt{J_1} \end{pmatrix}, \quad P \equiv \begin{pmatrix} p & q \\ q & s \end{pmatrix}.$$

In Eq. (3.21), the matrix  $T$  is a rotational matrix that diagonalizes the symmetric matrix  $Q \equiv J^{-1}P^{-1}J^{-1}$ , and it is defined by

$$T \equiv \begin{pmatrix} \cos \theta & \sin \theta \\ -\sin \theta & \cos \theta \end{pmatrix}.$$

The matrix  $Q$  is expressed as

$$Q = \frac{1}{\Delta} \begin{pmatrix} \frac{s}{J_2} & -\frac{q}{\sqrt{J_1 J_2}} \\ -\frac{q}{\sqrt{J_1 J_2}} & \frac{p}{J_1} \end{pmatrix}.$$

The rotational angle  $\theta$  is given by

$$\tan 2\theta = -\frac{2q\sqrt{J_1 J_2}}{J_1 s - J_2 p} \simeq -\frac{2\sqrt{2}}{5}\delta ab \simeq O(10^{-1}). \quad (3.22)$$

The eigenvalues of  $Q$ ,  $\nu_1$  and  $\nu_2$ , correspond to the frequencies of  $X$  and  $Y$ , respectively, and they are given as follows:

$$F \equiv TQT^{-1} = \begin{pmatrix} \nu_1^2 & 0 \\ 0 & \nu_2^2 \end{pmatrix}.$$

For  $a \simeq O(10) > b \simeq O(1)$ , by using Eqs. (2.1)–(2.3) for the parameters  $p$ ,  $q$  and  $s$ , the eigenvalues  $\nu_1$  and  $\nu_2$  are given as follows:

$$\nu_1^2 \simeq 5 \left( \frac{a^2}{a^2 + 6} + \delta^2 \frac{a^2}{6(1 - \frac{a^2}{b^2})} \right) \simeq 5, \quad (3.23)$$

$$\nu_2^2 \simeq 5 \left( \frac{b^2}{b^2 + 6} - \delta^2 \frac{a^2}{6(1 - \frac{a^2}{b^2})} \right) \simeq \frac{5b^2}{b^2 + 6}. \quad (3.24)$$

The equations of motion with respect to  $X$  and  $Y$  are given by

$$(D^2 + F + DRF) \begin{pmatrix} X \\ Y \end{pmatrix} = \begin{pmatrix} 0 \\ 0 \end{pmatrix},$$

where

$$R \equiv TJ^{-1}NJT^{-1}, \quad N \equiv \begin{pmatrix} \frac{1}{J_2\mu} & -n \\ n & \frac{1}{J_1\mu} \end{pmatrix}, \quad D \equiv \begin{pmatrix} \frac{d}{dt} & 0 \\ 0 & \frac{d}{dt} \end{pmatrix}.$$

The matrix  $R$  has components  $a_i$  as follows:

$$R = \begin{pmatrix} a_1 & a_2 \\ a_3 & a_4 \end{pmatrix}, \quad (3.25)$$

where  $a_i$  are defined by

$$a_1 \equiv m_1 - nk_1, \quad a_2 \equiv -m_2 - nk_2, \quad a_3 \equiv -m_3 + nk_3, \quad a_4 \equiv m_4 + nk_4. \quad (3.26)$$

In these equations,  $k_i$  are given by

$$k_1 \equiv -\nu_1^2 \sin \theta \cos \theta (f - f^{-1}) \simeq a^2 \delta \simeq O(1), \quad (3.27)$$

$$k_2 \equiv \nu_2^2 (f \sin^2 \theta + f^{-1} \cos^2 \theta) \simeq \frac{5b}{\sqrt{2}a} \simeq O(1), \quad (3.28)$$

$$k_3 \equiv \nu_1^2(f \cos^2 \theta + f^{-1} \sin^2 \theta) \simeq \frac{5a}{\sqrt{2}b} \simeq O(10), \quad (3.29)$$

$$k_4 \equiv -\nu_2^2 \sin \theta \cos \theta (f - f^{-1}) \simeq \frac{\delta a^2}{2} \simeq O(1), \quad (3.30)$$

and  $m_i$  depending on the friction parameter  $\mu$  are given as follows:

$$m_1 \equiv \frac{f}{J_2 \mu} \frac{\nu_1^2}{\nu_2^2} k_2 \simeq \frac{5\sqrt{b^2 + 6} k_2}{ab^2 \mu}, \quad (3.31)$$

$$m_2 \equiv \frac{f}{J_2 \mu} k_4 \simeq \frac{5k_4}{a\sqrt{b^2 + 6}\mu}, \quad (3.32)$$

$$m_3 \equiv \frac{f}{J_2 \mu} k_1 \simeq \frac{5k_1}{a\sqrt{b^2 + 6}\mu}, \quad (3.33)$$

$$m_4 \equiv \frac{f}{J_2 \mu} \frac{\nu_2^2}{\nu_1^2} k_3 \simeq \frac{5\sqrt{b^2 + 6} k_3}{ab^2 \mu}, \quad (3.34)$$

where  $f$  is defined by

$$f \equiv \sqrt{\frac{J_2}{J_1}} = \sqrt{\frac{a^2 + 6}{b^2 + 6}}, \quad (3.35)$$

and approximation equations such as

$$\frac{f\nu_1^2}{J_2\nu_2^2} \simeq \frac{5\sqrt{b^2 + 6}}{ab^2}, \quad \frac{f}{J_2} \simeq \frac{5}{a\sqrt{b^2 + 6}} \quad (3.36)$$

are used.

Finally, the effective equations of motion are obtained as follows:

$$\ddot{X} + \nu_1^2 X + a_1 \dot{X} + a_2 \dot{Y} = 0, \quad (3.37)$$

$$\ddot{Y} + \nu_2^2 Y + a_3 \dot{X} + a_4 \dot{Y} = 0, \quad (3.38)$$

$$I_3 \dot{n} - (X, Y) (KD^2 - K - SD) \begin{pmatrix} X \\ Y \end{pmatrix} = 0. \quad (3.39)$$

Here,  $S$  and  $K$  are  $2 \times 2$  matrices as follows:

$$K \equiv \begin{pmatrix} k_1 & -k_3 \\ k_2 & -k_4 \end{pmatrix}, \quad S \equiv \begin{pmatrix} s_1 & s_2 \\ s_3 & s_4 \end{pmatrix}, \quad (3.40)$$

where  $s_i$  are defined by

$$s_1 \equiv \nu_1^2 \left( n\sqrt{J_1 J_2} k_3 - \frac{k_1}{\mu} \right),$$

$$s_2 \equiv \nu_2^2 \left( n\sqrt{J_1 J_2} k_1 + \frac{k_3}{\mu} \right),$$

$$s_3 \equiv \nu_1^2 \left( n\sqrt{J_1 J_2} k_4 - \frac{k_2}{\mu} \right),$$

$$s_4 \equiv \nu_2^2 \left( n\sqrt{J_1 J_2} k_2 + \frac{k_4}{\mu} \right).$$

From Eqs. (3.31)–(3.34), it is found that these  $m_i$  are approximated as  $m_i \simeq \frac{5k_i}{ab\mu}$ . Thus,  $m_i$  take a value of the order  $O(10^{-2})$  or  $O(10^{-1})$ , because  $k_i$  take an order  $O(1)$  or  $O(10)$  from Eqs. (3.27)–(3.30) when  $\frac{1}{\mu} \simeq O(10^{-2})$  is considered. Furthermore, when  $n \simeq O(10^{-2})$  is considered, the order

of the  $nk_i$  value becomes  $O(10^{-2})$  or  $O(10^{-1})$ . After all, the maximal value of parameters  $a_i$  is estimated at order  $O(10^{-1})$ . Thus the quantities of  $O(a_i^2)$  are neglected in the next section.

For the no-slip case ( $\mu$  is sufficiently large),

$$m_i \simeq 0. \quad (3.41)$$

Thus, it is observed that the effect of friction is included as  $\frac{1}{\mu}$  in the parameters  $m_i$ .

#### 4. A SLOWLY VARYING MODE

The motion of a rattleback contains a rapid frequency rattling mode and a slowly varying amplitude mode. To discuss the number of spin reversals, the slowly varying mode should be analyzed. In this section, by approximately solving the characteristic equation and considering the time average of the rapid frequency mode, the equations of the slowly varying mode are derived from the effective equations of motion which were obtained in the previous section.

To study the mode contained in  $X(t)$  and  $Y(t)$ , the characteristic equation given in Eqs. (3.37) and (3.38) is approximately solved. In this case,  $n$  is considered to be a constant, because  $\dot{n}$  is a second-order term from Eq. (3.20). Moreover, the quantities of  $O(a_i^2)$  are neglected as explained in the previous section.

Two modes are observed, which correspond to the rattling motion of the long axial direction  $e^{i\nu_1 t} e^{-\frac{a_1}{2}t}$  and the short axial direction  $e^{i\nu_2 t} e^{-\frac{a_2}{2}t}$ . Then, the mode expansions of  $X(t)$  and  $Y(t)$  are given by

$$\begin{aligned} X(t) &= c_1 e^{i\lambda_1 t} + c_1^* e^{-i\lambda_1^* t} + c_2 e^{i\lambda_2 t} + c_2^* e^{-i\lambda_2^* t}, \\ Y(t) &= d_1 e^{i\lambda_1 t} + d_1^* e^{-i\lambda_1^* t} + d_2 e^{i\lambda_2 t} + d_2^* e^{-i\lambda_2^* t}, \end{aligned}$$

where  $\lambda_1 \equiv \nu_1 + i\frac{a_1}{2}$ ,  $\lambda_2 \equiv \nu_2 + i\frac{a_2}{2}$ , and  $*$  indicates a complex conjugate. The coefficients  $c_1$ ,  $c_2$ ,  $d_1$  and  $d_2$  are obtained from  $X(t)$  satisfying the equation of motion (Eq. (3.37)) and initial conditions such as  $X(0) = x_0$ ,  $Y(0) = y_0$ ,  $\dot{X}(0) = 0$  and  $\dot{Y}(0) = 0$  as follows:

$$\begin{aligned} c_1 &\simeq \left( \frac{1}{2} - i\frac{a_1}{4\nu_1} \right) x_0 + i\frac{a_2\nu_2^2}{2\nu_1\Delta} y_0, & c_2 &\simeq -i\frac{a_2\nu_2}{2\Delta} y_0, \\ d_1 &\simeq -i\frac{a_1^2}{8a_2\nu_1} x_0, & d_2 &\simeq -i\frac{a_1^2}{8a_2\nu_2} x_0 + \left( \frac{1}{2} - i\frac{a_2}{4\nu_2} \right) y_0, \end{aligned}$$

where  $\Delta \equiv \nu_1^2 - \nu_2^2$ . In order to obtain the behavior of  $n(t)$ , the method of time averaging of the terms in the rapidly varying mode such as  $e^{i\nu_i t}$  is adopted. This rapidly varying mode is contained in terms, such as  $X^2$  and  $X\dot{X}$ , of the equation for  $\dot{n}(t)$ . When the variables are given by  $Q_1(t) = F_1(t)S_1(t)$  and  $Q_2(t) = F_2(t)S_2(t)$ , (where  $F_i(t)$  are rapidly varying functions and  $S_i(t)$  are slowly varying functions such as  $e^{-\frac{a_i}{2}t}$ ), the time average of  $Q_1$  and  $Q_2$  ( $\langle Q_1 Q_2 \rangle$ ) is defined as follows:

$$\langle Q_1 Q_2 \rangle \equiv S_1 S_2 \lim_{T \rightarrow \infty} \frac{1}{T} \int_0^T F_1 F_2 dt.$$

Then, neglecting terms  $O(a_i^2)$ ,

$$\begin{aligned} \langle X^2 \rangle &\simeq \frac{x_0^2}{2} e^{-a_1 t}, & \langle X\dot{X} \rangle &\simeq -\frac{x_0^2}{4} a_1 e^{-a_1 t}, & \langle X\ddot{X} \rangle &\simeq -\frac{\nu_1^2 x_0^2}{2} e^{-a_1 t}, \\ \langle X\dot{Y} \rangle &\simeq \frac{a_1^2}{8a_2} x_0^2 e^{-a_1 t} - \frac{a_2\nu_2^2}{2\Delta} y_0^2 e^{-a_2 t} \simeq -\langle Y\dot{X} \rangle, & \langle XY \rangle &\simeq 0, & \langle X\dot{Y} \rangle &\simeq 0, \\ \langle Y^2 \rangle &\simeq \frac{y_0^2}{2} e^{-a_2 t}, & \langle Y\dot{Y} \rangle &\simeq -\frac{y_0^2}{4} a_2 e^{-a_2 t}, & \langle Y\ddot{Y} \rangle &\simeq -\frac{\nu_2^2 y_0^2}{2} e^{-a_2 t}. \end{aligned}$$

From these equations, it is observed that  $\langle X\dot{X} \rangle$  and  $\langle Y\dot{Y} \rangle$  are  $O(a_i)$ . Thus, the main part of  $\dot{n}$  is obtained as follows:

$$\begin{aligned} I_3\dot{n}(t) &\simeq k_1(\langle X\ddot{X} \rangle - \langle X^2 \rangle) - k_4(\langle Y\ddot{Y} \rangle - \langle Y^2 \rangle) \\ &= -\frac{k_1}{2}A^2 + \frac{k_4}{2}B^2, \end{aligned} \quad (4.1)$$

where

$$A \equiv \sqrt{\nu_1^2 - 1x_0}e^{-\frac{a_1}{2}t}, \quad B \equiv \sqrt{\nu_2^2 - 1x_0}e^{-\frac{a_4}{2}t}. \quad (4.2)$$

From the definitions given in Eq. (4.2), these variables satisfy the differential equations by using the approximation  $\dot{n} \simeq 0$  as follows:

$$\dot{A} = -\frac{a_1}{2}A, \quad \dot{B} = -\frac{a_4}{2}B. \quad (4.3)$$

In the no-slip case ( $\mu$  is sufficiently large), from Eq. (3.41), the parameters  $a_1$  and  $a_4$  are given as  $a_1 = -nk_1$  and  $a_4 = nk_4$ , respectively. Then, substituting these parameters into Eqs. (4.1) and (4.3) gives equations that correspond to those obtained by Pascal [2], Markeev [3] and Moffatt and Tokieda [5].

Multiplying Eq. (4.1) by  $n$  and using Eqs. (3.26) and (4.3), the following equation is obtained:

$$\frac{d}{dt}(N^2 + A^2 + B^2) = -m_1A^2 - m_4B^2, \quad (4.4)$$

where  $N \equiv \sqrt{I_3}n$ . For the no-slip case ( $m_i = 0$ ), the variable  $E_1 \equiv N^2 + A^2 + B^2$  corresponds to the sum of energy about the rotation  $N$ , and the amplitudes of the long and short axial directions ( $A$  and  $B$ , respectively) are conserved. Moreover, from Eq. (4.3), it is observed that the variable  $E_2 \equiv A^\gamma B$  is conserved, where  $\gamma \equiv \frac{k_4}{k_1}$ . In the phase spaces of  $N$ ,  $A$  and  $B$ ,  $E_1$  corresponds to a sphere and  $E_2$  corresponds to a quasi-hyperbolic cylinder. The trajectories of the system are closed curves that intersect this cylindrical surface and the sphere. Therefore, an infinite number of spin reversals is obtained.

In contrast, for the slip case, it is observed that the energy  $E_1$  decreases according to the right-hand-side of Eq. (4.4), which relates to friction. By using the approximation  $\dot{n} \simeq 0$ , it is assumed that  $\gamma$  is almost constant and  $E_2$  is almost conserved; then, the trajectory of the system decreases as the radius of the sphere of  $E_1$  decreases. Therefore, a finite number of spin reversals is obtained.

## 5. A NEW PHENOMENON FOR THE SLIP CASE

For the no-slip case, rattle vibration increases irrespective of how small the initial spin  $n_0$  is, and in theory, spin reversal occurs. However, for the slip case, when  $n_0$  is small, vibration does not increase, and rotation stops. Even if rattle vibration occurs, spin reversal does not. Thus, a critical value of the spin  $n_{c1}$  may exist under which rattle vibration does not increase, and a critical value of the spin  $n_{c2}$  may exist under which rattle vibration increases but spin reversal does not occur. Therefore, it is assumed that the number of spin reversals is finite due to the existence of these critical spin values. In this section, some new facts relating to these values are discussed.

### 5.1. Critical Spin $n_{c1}$ Necessary to Increase Rattle Vibration

For spin reversal to occur, rattle vibration must increase. This vibration increases according to the factor  $e^{-a_1t}$  and  $e^{-a_4t}$ . For the no-slip case, these factors are  $e^{+nk_1t}$  and  $e^{-nk_4t}$ . From Eqs. (3.27) and (3.30), it is observed that  $nk_1$  and  $nk_4$  have the same sign and if one mode increases, the other decreases. In contrast, for the slip case,  $m_1$  and  $m_4$  are in  $a_1$  and  $a_4$ ; hence,  $a_1 > 0$  and  $a_4 > 0$  occur according to the value of  $n$ . In this case, both modes decrease, and rattle vibration does not increase. The spin values  $n_{c1\pm}$  are given by

$$\begin{aligned} n_{c1+} &\equiv \frac{m_1}{k_1} = -\frac{\cos^2 \theta + f^2 \sin^2 \theta}{J_2 \mu \sin \theta \cos \theta (f - f^{-1})}, \\ n_{c1-} &\equiv -\frac{m_4}{k_4} = \frac{f^2 \cos^2 \theta + \sin^2 \theta}{J_2 \mu \sin \theta \cos \theta (f - f^{-1})}, \end{aligned}$$

for  $k_1 > 0$ . For the case of  $k_1 < 0$ , these values reverse and are given by  $n_{c1+} = -\frac{m_4}{k_4}$  and  $n_{c1-} = \frac{m_1}{k_1}$ . Therefore, it is observed that rattle vibration decreases for the initial spin  $n_0$  in the range  $n_{c1-} < n_0 < n_{c1+}$ .

### 5.2. Critical Spin $n_{c2}$ Necessary to Reverse Rattleback Spin

When the spin is more than  $n_{c1}$ , rattle vibration increases. However, the spin does not necessarily reverse. A critical spin value  $n_{c2}$  may exist over which spin reversal occurs.

When starting with  $n_0 > 0$ , although it is near the value of  $n_0$ , for a while, rattle vibration begins rapidly, and spin decreases. Eventually, the rattleback stops spinning and then reverses direction, and the spin value decreases to  $n_1 < 0$ . This spin value  $n_1$  is obtained as follows.

Now, consider the case for  $k_1 > 0$ ,  $k_4 > 0$  and  $n_0 > 0$ . At first, the modes  $A$  and  $B$  exponentially increase and decrease, respectively: therefore, from Eq. (4.1),  $\dot{n}$  approximates to

$$I_3 \dot{n} \simeq -\frac{k_1 \nu_1^2}{2} A^2. \quad (5.1)$$

Integrating this equation from  $t_0 (n = n_0 > 0)$  to  $t_1 (n = n_1)$  gives

$$I_3 (n_1 - n_0) = -\frac{k_1 \nu_1^2}{2} \int_{t_0}^{t_1} A^2. \quad (5.2)$$

Furthermore, Eq. (4.4) approximates to

$$\frac{d}{dt} (I_3 n^2 + \nu_1^2 A^2) \simeq -m_1 \nu_1^2 A^2. \quad (5.3)$$

Integrating this equation gives

$$\nu_1^2 \int_{t_0}^{t_1} A^2 \simeq -\frac{I_3}{m_1} (n_1^2 - n_0^2), \quad (5.4)$$

where it is considered that  $A(t_0) \simeq 0$  and  $A(t_1) \simeq 0$ . By substituting Eq. (5.4) into Eq. (5.2),  $n_1$  is given by

$$n_1 = -n_0 + \frac{2m_1}{k_1}. \quad (5.5)$$

Then it is observed that if  $n_1 < 0$ , that is, the initial spin  $n_0 > \frac{2m_1}{k_1}$ , one spin reversal occurs, and if  $n_0 \leq \frac{2m_1}{k_1}$ , no spin reversal occurs. Therefore, it is observed that if  $n_{c1+} = \frac{m_1}{k_1} < n_0 \leq \frac{2m_1}{k_1}$ , rattle vibration increases but spin reversal does not occur. Similarly, when  $n_0 < 0$ , the condition  $n_0 < -\frac{2m_4}{k_4}$  must be satisfied for spin reversal to occur.

Finally, it is observed that there exist critical spins  $n_{c2\pm}$  as follows:

$$n_{c2+} \equiv \frac{2m_1}{k_1}, \quad n_{c2-} \equiv -\frac{2m_4}{k_4}.$$

When  $n_{c2-} \leq n_0 < n_{c1-}$  or  $n_{c1+} < n_0 \leq n_{c2+}$ , rattle vibration increases but spin reversal does not occur. For the case of  $k_1 < 0$ , it is observed that  $n_{c2-}$  and  $n_{c2+}$  are switched:  $n_{c2-} = \frac{2m_1}{k_1}$  and  $n_{c2+} = -\frac{2m_4}{k_4}$ .

### 5.3. The Number of Spin Reversals $n_r$

For the no-slip case, because dynamical energy is conserved, an infinite number of spin reversals occur. In contrast, for the slip case, because friction exists, the number of spin reversals  $n_r$  is finite.

As discussed in the previous section, for  $n_1 < 0$ , the condition for the first spin reversal occurrence is given by

$$\frac{1}{h_1} > 1, \quad (5.6)$$

where  $h_1$  is defined by

$$h_1 \equiv \left| \frac{2m_1}{k_1 n_0} \right|. \quad (5.7)$$

Next, for the second spin reversal, if  $n_1$  satisfy  $n_1 > n_{c1-} = -\frac{m_4}{k_4}$ , rattle vibration does not increase and the rattleback stops spinning. When  $n_1$  satisfy  $n_{c1-} > n_1 > n_{c2-} = -\frac{2m_4}{k_4}$ , rattle vibration increases but spin reversal does not occur. Therefore, the condition for the second spin reversal to occur is as follows:

$$n_1 < -\frac{2m_4}{k_4}. \quad (5.8)$$

Now, the spin value  $n_2$  after the second rattle vibration is estimated. Similar to the derivation of  $n_1$  in the previous section, the following equation is obtained:

$$\begin{aligned} n_2 &= -n_1 - \frac{2m_4}{k_4} \\ &= n_0 - \frac{2m_1}{k_1} - \frac{2m_4}{k_4}. \end{aligned}$$

Thus, if  $n_2 > 0$ , the second spin reversal occurs. This condition is consistent with Eq. (5.8). The condition for the second spin reversal occurrence is given by

$$\frac{1}{h_1} > 1 + \rho, \quad (5.9)$$

where

$$\rho \equiv \frac{h_4}{h_1}, \quad h_4 \equiv \left| \frac{2m_4}{k_4 n_0} \right|.$$

From Eqs. (5.6) and (5.9), the condition that spin reversal occurs only once is given by  $1 < \frac{1}{h_1} \leq 1 + \rho$ . Similarly, the condition that spin reversal occurs only two times is given by  $1 + \rho < \frac{1}{h_1} \leq 2 + \rho$ , and the condition that spin reversal occurs only three times is given by  $2 + \rho < \frac{1}{h_1} \leq 2 + 2\rho$ , and so on.

It is observed that the number of spin reversals  $n_r$  satisfies the following inequalities:

I.  $n_0 > 0, k_1 > 0, k_4 > 0$  or  $n_0 < 0, k_1 < 0, k_4 < 0$

$$K_0(n_r - 1, \rho) < \frac{1}{h_1} \leq K_0(n_r, \rho), \quad (5.10)$$

II.  $n_0 > 0, k_1 < 0, k_4 < 0$  or  $n_0 < 0, k_1 > 0, k_4 > 0$

$$K_1(n_r - 1, \rho) < \frac{1}{h_1} \leq K_1(n_r, \rho), \quad (5.11)$$

where

$$\begin{aligned} K_0(n, \rho) &\equiv \sum_{i=0}^n P_+(i) + P_-(i)\rho, \\ K_1(n, \rho) &\equiv \sum_{i=0}^n P_+(i)\rho + P_-(i), \\ P_{\pm}(i) &\equiv \frac{1 \pm (-1)^i}{2}. \end{aligned}$$

Finally, from the inequalities stated in Eqs. (5.10) and (5.11), the number of spin reversals  $n_r$  is obtained.

For case (I),  $n_r$  is given by

$$n_r = \begin{cases} 2[x] + 1 & \text{if } x - 1 \leq [x] < x - \frac{1}{1+\rho} \\ 2[x] & \text{if } x - \frac{1}{1+\rho} \leq [x] < x \end{cases} \quad (5.12)$$

and for case (II),  $n_r$  is given by

$$n_r = \begin{cases} 2[x] + 1 & \text{if } x - 1 \leq [x] < x - 1 + \frac{1}{1+\rho} \\ 2[x] & \text{if } x - 1 + \frac{1}{1+\rho} \leq [x] < x \end{cases} \quad (5.13)$$

where  $x$  is defined by

$$x \equiv \frac{1}{h_1(\rho + 1)},$$

and  $[x]$  is Gauss' symbol, which represents the greatest integer less than or equal to  $x$ .

#### 5.4. Relationship Between the Number of Spin Reversals and the Rattleback's Shape

In this subsection, the relationship between the number of spin reversals, the axis inclination ( $\delta \simeq \theta$  in Eq. (3.22)), the coefficient of friction  $\mu$  and the rattleback's shape is obtained.

The factor  $x = \frac{1}{h_1(\rho+1)}$  is written as

$$x = \frac{1}{2} J_2 \mu |n_0 \sin \theta \cos \theta| L(f),$$

where  $L(f)$  is the form factor given by

$$L(f) \equiv \frac{|f - f^{-1}|}{1 + f^2}. \quad (5.14)$$

This expression shows that the number of spin reversals is proportional to the coefficient of friction  $\mu$ , the axis inclination  $\delta$ , and the initial spin  $n_0$ . Therefore, when the friction is large (close to the no-slip case) and the asymmetry between the shape axes and the principal inertia axes is large, the number of spin reversals becomes large. Here, it is found that the form factor  $L(f)$  plays an important role in determining the relation between the shape of the rattleback and the number of spin reversals. When the long axis  $a$  is fixed, which corresponds to a fixed  $J_2$ , enlarging  $f$  corresponds to reduction in  $J_1$  from Eq. (3.35). Furthermore, from Eq. (3.14), reducing  $J_1$  corresponds to a reduction in  $b$ , which indicates that the rattleback becomes long and slender. In contrast, reducing  $f$  results in the rattleback becoming more circular, such as  $J_1 = J_2$ . The form factor  $L(f)$  has maximum at  $f = \sqrt{2 + \sqrt{5}}$ . Thus, it is observed that if the rattleback becomes long and slender, rattle vibration about the short axis does not easily occur and the number of spin reversals is reduced. This also occurs if the rattleback is more circular. The relationship between  $a$  and  $b$  corresponding to the maximum of  $f$  is given by

$$b^2 = \frac{a^2 + 6}{2 + \sqrt{5}} - 6. \quad (5.15)$$

For example, if  $a = 10$ ,  $b$  becomes approximately 4.4. Figure 3 shows the change in the form factor  $L(f)$  when  $a = 10$  is fixed and  $b$  is varied from 1 to 10. It is observed that there is a maximum value around  $b \simeq 4.4$ .

## 6. NUMERICAL RESULTS

In this section, the results of computations based on the exact system described in Eqs. (2.6)–(2.10) are presented and compared with those based on the effective equations of motion described in Eqs. (3.37)–(3.39).

For the numerical simulations, the NDSolve command in *Mathematica* is used.

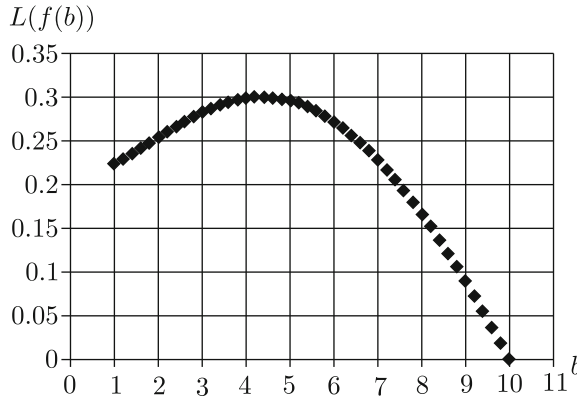


Fig. 3. The form factor  $L(f)$  versus  $b$  for  $a = 10$ .

6.1. Validity of the Approximation  $\dot{v}_0 \gg \dot{v}_p$

In Section 3, the approximation  $\dot{v}_0 \gg \dot{v}_p$  was used to derive effective equations of motion.

The initial conditions are  $x_0 = y_0 = 0.01$ ,  $\dot{x}_0 = \dot{y}_0 = 0$  and  $n_0 = 0.05$  with parameters  $a = 10$ ,  $b = 3$ , and  $\delta = 0.03$ . Figure 4 shows the behavior of  $\dot{v}_{01}$  and  $\dot{v}_{p1}$  for  $\mu = 100$ , and Fig. 5 shows the behavior of  $\dot{v}_{02}$  and  $\dot{v}_{p2}$  for  $\mu = 100$ . From Figs. 4 and 5, the comparison of the amplitudes

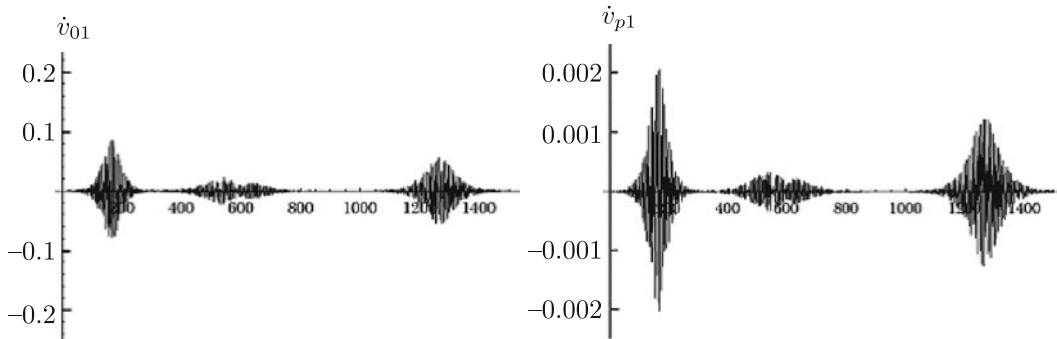


Fig. 4. Time evolution of  $\dot{v}_{01}$  and  $\dot{v}_{p1}$  for  $\mu = 100$ .

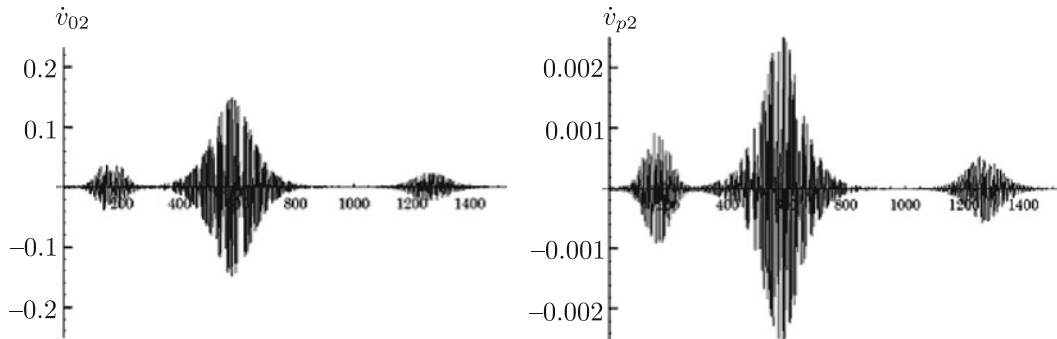


Fig. 5. Time evolution of  $\dot{v}_{02}$  and  $\dot{v}_{p2}$  for  $\mu = 100$ .

shows that  $\dot{v}_{p1} \simeq \dot{v}_{01} \times \frac{1}{50}$  and  $\dot{v}_{p2} \simeq \dot{v}_{02} \times \frac{1}{50}$ . Thus, it can be safely assumed that  $\dot{v}_{01} \gg \dot{v}_{p1}$  and  $\dot{v}_{02} \gg \dot{v}_{p2}$ . Figures 6 and 7 are the same as Figs. 4 and 5, respectively, but for  $\mu = 200$ . In this case, it is similarly shown that  $\dot{v}_{p1} \simeq \dot{v}_{01} \times \frac{1}{100}$  and  $\dot{v}_{p2} \simeq \dot{v}_{02} \times \frac{1}{100}$ . Thus,  $\dot{v}_{01} \gg \dot{v}_{p1}$  and  $\dot{v}_{02} \gg \dot{v}_{p2}$ . Note that the approximation improves when  $\mu$  increases. After all, it is concluded that the approximation  $\dot{v}_0 \gg \dot{v}_p$  is valid.

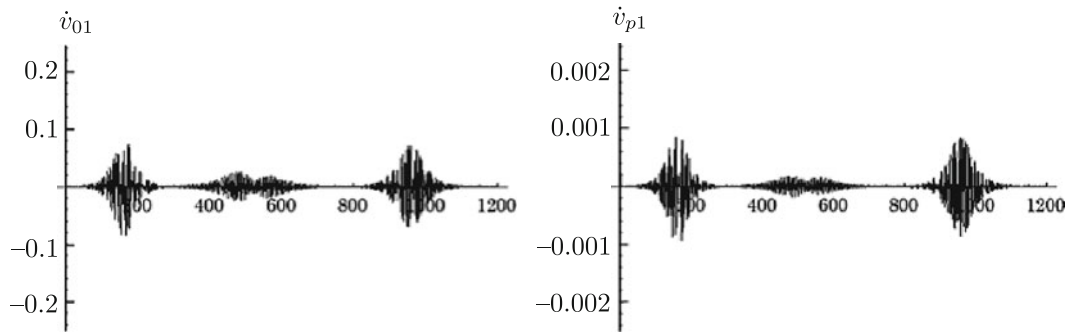


Fig. 6. Time evolution of  $\dot{v}_{01}$  and  $\dot{v}_{p1}$  for  $\mu = 200$ .

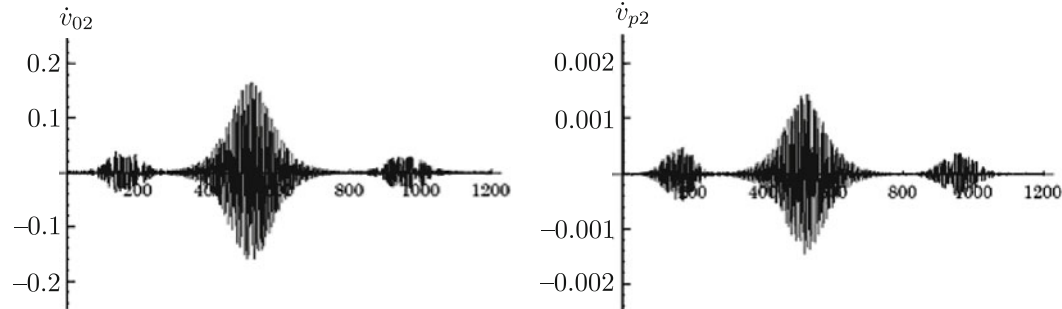


Fig. 7. Time evolution of  $\dot{v}_{02}$  and  $\dot{v}_{p2}$  for  $\mu = 200$ .

### 6.2. $n_{c1\pm}$ , $n_{c2\pm}$ , and Spin Reversal Behavior

In Sections 5.1 and 5.2, the critical values of spin necessary to increase rattle vibration and cause spin reversal are obtained. Here, computational results for these values and the spin reversal behavior which are obtained from a simulation based on the exact system are presented.

The initial conditions are  $x_0 = y_0 = 0.01$ , and  $\dot{x}_0 = \dot{y}_0 = 0$  with parameters  $a = 10$ ,  $b = 3$ , and  $\delta = 0.03$ . The coefficient of friction is set to  $\mu = 75$ . For these initial conditions, the following critical values of spin are obtained:  $n_{c2+} = 0.00358$ ,  $n_{c1+} = 0.00179$ ,  $n_{c1-} = -0.01$ , and  $n_{c2-} = -0.0201$ . Figure 8 shows the computed evolution of  $n(t)$ . In Fig. 8a, as discussed in Section 5.1, the dotted line with the initial spin  $n_0 = 0.0015 < n_{c1+}$  shows that rattle vibration does not increase. As discussed in Section 5.2, the dashed line with the initial spin  $n_{c1+} < n_0 = 0.003 < n_{c2+}$  shows that rattle vibration increases but spin reversal does not occur. The solid line with the initial spin  $n_{c2+} < n_0 = 0.005$  shows that the spin reversal behavior agrees with that discussed in Section 5.2. Figure 8b shows the behavior of  $n(t)$  for negative initial spins  $n_0 = -0.006$  (dotted line),  $-0.015$  (dashed line), and  $-0.025$  (solid line). Even if the initial spin is negative, the same behavior occurs about  $n_{c1-}$  and  $n_{c2-}$ . Thus, it is observed that spin reversal behaviors are dependent on these critical values.

### 6.3. The Number of Spin Reversals $n_r$ and the Friction Coefficient $\mu$

This subsection discusses how the number of spin reversals  $n_r$  changes depending on the friction coefficient  $\mu$ . This number of spin reversals is obtained from a simulation based on the exact system described in Eqs. (2.6)–(2.10).

The initial conditions are  $x_0 = y_0 = 0.01$ ,  $\dot{x}_0 = \dot{y}_0 = 0$ , and  $n_0 = 0.05$  with parameters  $a = 10$ ,  $b = 3$ , and  $\delta = 0.03$ . Figure 9a shows the behavior of  $n(t)$  for  $\mu = 60$  (solid line), 130 (dotted line) and 200 (dashed line). It is observed that for each of these  $\mu$  values, the number of spin reversals increases to three, six, and nine times, respectively. Figure 9b shows the behavior of spin  $n(t)$  for  $\mu = 500$  (solid line), 1000 (dotted line), 1500 (dashed line). Note that the spin behavior is similar to that for the no-slip case as the friction increases.

We usually consider that when friction increases, the energy loss becomes large, so that the reverse number decreases. The numerical simulations show the opposite thing to this intuition. In

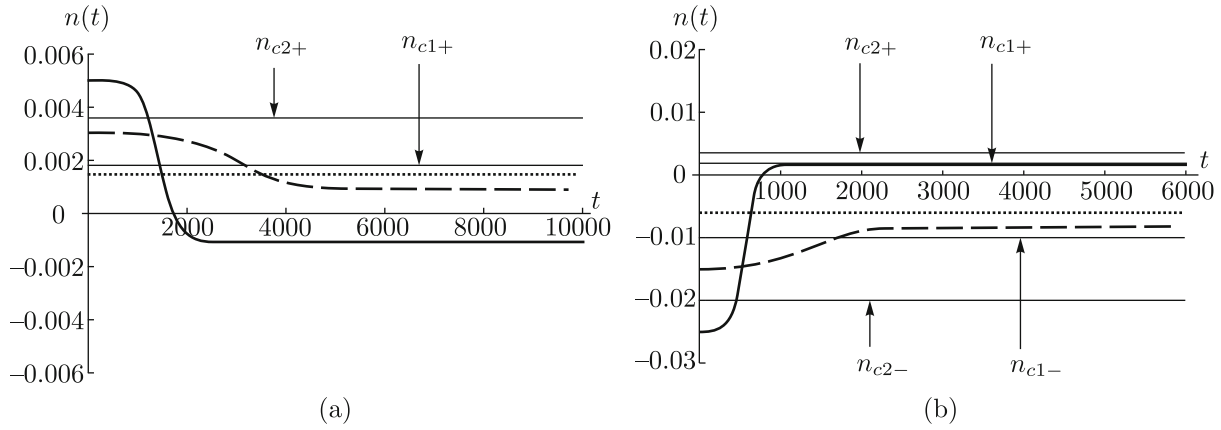


**Fig. 8.** Time evolution of  $n(t)$  with (a) positive initial spin with  $n_0 = 0.0015$  (dotted line), 0.003 (dashed line), and 0.005 (solid line) and (b) negative initial spin with  $n_0 = -0.006$  (dotted line),  $-0.015$  (dashed line) and  $-0.025$  (solid line).

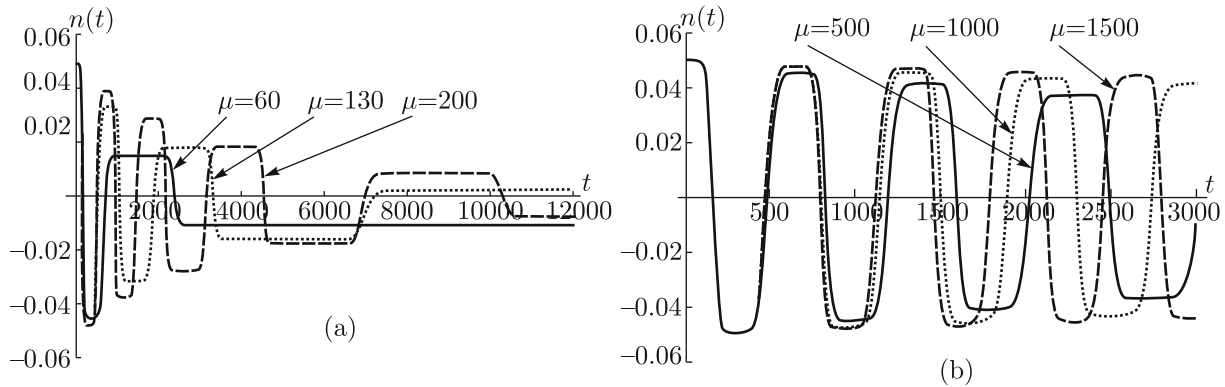


**Fig. 9.** Time evolution of  $n(t)$ . (a) The initial values of  $\mu$  are 60 (solid line), 130 (dotted line), and 200 (dashed line). (b) The initial values of  $\mu$  are 500 (solid line), 1000 (dotted line), and 1500 (dashed line).

reality, the contact with the horizontal plane is not a point but an area, spinning torque due to rotation  $n$  seems to effect the dynamics of rattleback as discussed by Garcia and Hubbard [12]. The adopted model does not include this spinning torque, so that the energy loss depends only on the velocity  $\mathbf{v}_p$  which becomes small when the friction coefficient  $\mu$  becomes large, thus, it may be considered that the number of spin reversals increases. Moreover, in reality, when the spin reversal does not occur, the contact point  $x_p$  settles down to  $x = y = 0$  and  $z = 1$ , and the slip velocity  $\mathbf{v}_p$  is equal to zero. Then, the rattleback stops spinning after a while. In contrast, in the numerical simulation, if we set the conditions  $\mathbf{v}_p = 0$ ,  $\ddot{x} = \dot{x} = x = 0$ , and  $\ddot{y} = \dot{y} = y = 0$ ,  $\dot{n}$  becomes zero from Eq. (3.15). Therefore, the spin  $n(t)$  becomes constant and does not stop after the spin reversal ends, as shown in Fig. 9a. It is considered that these phenomena are also dependent on not considering spinning torque due to the frictional force by spinning.

#### 6.4. The Approximate Number of Spin Reversals $n_{r:ap}$ Versus the Exact Number of Spin Reversals $n_{r:ex}$

In this section, the approximate number of spin reversals  $n_{r:ap}$  obtained from Eqs. (5.12) and (5.13) in Section 5.3 is compared with the exact number of spin reversals  $n_{r:ex}$  obtained from a simulation based on the exact system described in Eqs. (2.6)–(2.10).

The initial conditions are  $x_0 = y_0 = 0.01$ ,  $\dot{x}_0 = \dot{y}_0 = 0$  and  $n_0 = 0.05$  with parameters  $a = 10$ ,  $b = 3$ , and  $\delta = 0.03$ . Figure 10 shows the number of spin reversals  $n_r$  for a range of values of  $\mu$  from 20 to 200. Crosses represent  $n_{r:ex}$  and the boxes represent  $n_{r:ap}$ . Up to  $\mu \simeq 70$ , both values are

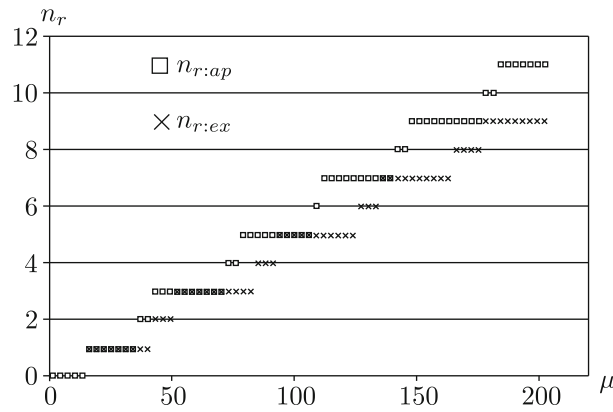


Fig. 10. The number of spin reversals  $n_r$  versus  $\mu$ :  $\square$  represents  $n_{r:ap}$  and  $\times$  represents  $n_{r:ex}$ .

almost identical, but the difference increases as  $\mu$  increases. It is assumed that the terms neglected in the approximation affect energy dissipation. Thus, for a given value of  $\mu$ ,  $n_{r:ap}$  is larger than  $n_{r:ex}$ .

### 6.5. The Form Factor $L(f)$ and $n_{r:ex}$

This section discusses the relationship between the form factor defined in Eq. (5.14) and  $n_{r:ex}$ .

The initial conditions are  $x_0 = y_0 = 0.01$ ,  $\dot{x}_0 = \dot{y}_0 = 0$ , and  $n_0 = 0.05$  with parameters  $a = 10$ , and  $\delta = 0.03$ . Figure 11 shows the behavior of  $n_{r:ex}$  as a function of the parameter  $b$  for  $\mu = 100$  and 200. Note that the  $b$  dependence of  $n_{r:ex}$  is similar to that of the form factor presented in Fig. 3. Therefore, the estimate derived from the effective equations of motion is qualitatively correct.

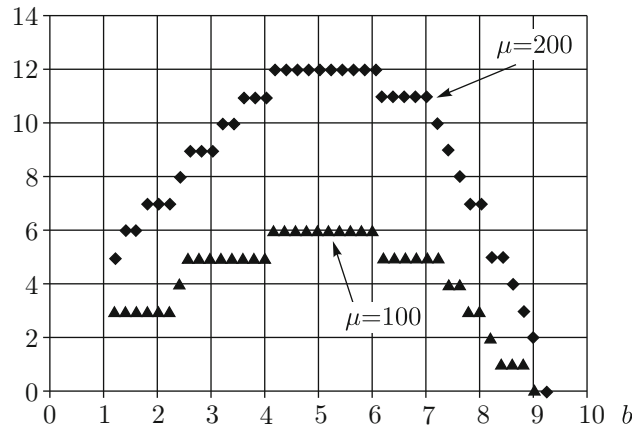


Fig. 11. The number of spin reversals  $n_{r:ex}$  versus  $b$ .

## 7. DISCUSSION AND CONCLUSIONS

In this paper, in order to answer the questions mentioned in the introduction, the behavior of a rattleback with viscous friction is examined.

The following results have been established analytically and confirmed numerically.

Critical values of the initial spin exist:  $n_{c1\pm}$  and  $n_{c2\pm}$ . When the initial spin  $n_0$  is in the region  $n_{c1-} < n_0 < n_{c1+}$ , rattle vibration does not increase. When the initial spin  $n_0$  is in the region  $n_{c2-} < n_0 < n_{c1-}$  or  $n_{c1+} < n_0 < n_{c2+}$ , rattle vibration increases but spin reversal does not occur. A numerical simulation based on the exact equations of motion has confirmed the existence of these values.

The number of spin reversals  $n_r$  is theoretically obtained as a function of the coefficient of friction  $\mu$  and the form factor  $L(f)$ , which contains the ratio of  $a$  to  $b$ .

From the expression of  $n_r$ , it was found that the number of spin reversals increases as  $\mu$  increases and a certain value of the ratio of  $a$  to  $b$  gives the maximum number of spin reversals.

In this paper, viscous friction is adopted to perform a first examination of spin reversal. However, in reality it is assumed that spin reversal is associated with the effect of Coulomb friction.

Furthermore, it seems that rolling friction and friction by spinning are also effective. Therefore, these frictions should be adopted to further understand the rattleback behavior. This is a subject for future investigations.

#### ACKNOWLEDGMENTS

I thank members of the elementary particle physics groups at Niigata University and Yamagata University for their valuable comments on my study in an autumn seminar at Bandai Fukushima in Japan (2010). I also appreciate the support received at a workshop hosted by the Yukawa Institute for Theoretical Physics at Kyoto University.

#### REFERENCES

1. Walker, G. T., On a Dynamical Top, *Q. J. Pure Appl. Math.*, 1896, vol. 28, pp. 175–185.
2. Pascal, M., Asymptotic Solution of the Equations of Motion for a Celtic Stone, *Prikl. Mat. Mekh.*, 1983, vol. 47, no. 2, pp. 321–329 [*J. Appl. Math. Mech.*, 1983, vol. 47, no. 2, pp. 269–276].
3. Markeev, A. P., The Dynamics of a Rigid Body on an Absolutely Rough Plane, *Prikl. Mat. Mekh.*, 1983, vol. 47, no. 4, pp. 575–582 [*J. Appl. Math. Mech.*, 1983, vol. 47, no. 4, pp. 473–478].
4. Blackowiak, A. D., Rand, R. H., and Kaplan, H., The Dynamics of the Celt with Second Order Averaging and Computer Algebra, in *Proc. of the ASME DETC'97/VIB-4103*, 1997.
5. Moffatt, H. K. and Tokieda, T., Celt Reversals: A Prototype of Chiral Dynamics, *Proc. Roy. Soc. Edinburgh Sect. A*, 2008, vol. 138, no. 2, pp. 361–368.
6. Bondi, H., The Rigid Body Dynamics of Unidirectional Spin, *Proc. R. Soc. Lond. Ser. A Math. Phys. Eng. Sci.*, 1986, vol. 405, pp. 265–274.
7. Borisov, A. V. and Mamaev, I. S., Strange Attractors in Rattleback Dynamics, *Uspekhi Fiz. Nauk*, 2003, vol. 173, no. 4, pp. 408–418 [*Physics–Uspekhi*, 2003, vol. 46, no. 4, pp. 393–403].
8. Borisov, A. V., Kilin, A. A., and Mamaev, I. S., New Effects in Dynamics of Rattlebacks, *Dokl. Phys.*, 2006, vol. 51, no. 5, pp. 272–275.
9. Borisov, A. V., Jalnina, A. Yu., Kuznetsov, S. P., Sataev, I. R., and Sedova, J. V., Dynamical Phenomena Occurring due to Phase Volume Compression in Nonholonomic Model of the Rattleback, *Regul. Chaotic Dyn.*, 2012, vol. 17, no. 6, pp. 512–532.
10. Kane, T.R. and Levinson, D.A., Realistic Mathematical Modeling of the Rattleback, *Int. J. Nonlinear Mech.*, 1982, vol. 17, no. 3, pp. 175–168.
11. Lindberg, R. E. Jr. and Longman, R. W., On the Dynamic Behavior of the Wobblestone, *Acta Mech.*, 1983, vol. 49, nos. 1–2, pp. 81–94.
12. Garcia, A. and Hubbard, M., Spin Reversal of the Rattleback: Theory and Experiment, *Proc. R. Soc. Lond. Ser. A Math. Phys. Eng. Sci.*, 1988, vol. 418, no. 1854, pp. 165–197.
13. Karapetyan, A. V., On Realizing Nonholonomic Constraints by Viscous Friction Forces and Celtic Stones Stability, *Prikl. Mat. Mekh.*, 1981, vol. 45, no. 1, pp. 42–51 [*J. Appl. Math. Mech.*, 1981, vol. 45, no. 1, pp. 30–36].